MODELLING AND VALIDATION OF CATALYTIC HYDROGEN RECOMBINATION IN THE 3D CFD CODE GASFLOW II

P. Royl, J. R. Travis, W. Breitung

Forschungszentrum Karlsruhe
Institut für Kern- und Energietechnik, Germany

Abstract

During hypothetical core melt accidents steam and hydrogen can be released into the air filled containment of pressurized water reactors (PWR). Without counter measures flammable mixtures may form and cause combustion loads that could threaten the integrity of the containment. German PWR's are now equipped with passive catalytic recombiners so called PARs (passive autocatalytic recombiners). They are arranged in boxes with arrays of plates coated with a platinum catalyst and are designed to prevent the accumulation of detonable conditions. Recombiner models have been implemented into the CFD code GASFLOW II to simulate such PAR mitigation in thermal hydraulic full containment calculations for various accident scenarios. After a brief description of these models this contribution will give the results from validation calculations of these models with a 3D experiment for plate recombiners (HDR test E11.8.1) and the thermal hydraulic analysis of larger scale experiments which investigated the performance of such box recombiners with steam/hydrogen release under realistic accident conditions.

SAMPLE ABSTRACT PAGE

Introduction

During hypothetical core melt accidents steam and hydrogen can be released into the air filled containment of pressurized water reactors (PWR). Without counter measures flammable mixtures may form and cause combustion loads that could threaten the integrity of the containment. German PWR's are now equipped with passive catalytic recombiners so called PARs (passive autocatalytic recombiners). They are arranged in boxes with arrays of plates coated with a platinum catalyst and are designed to prevent the accumulation of detonable conditions. Recombiner models have been implemented into the CFD code GASFLOW II [1] to simulate such PAR mitigation in thermal hydraulic full containment calculations for various accident scenarios. The recombiners operate in the 3D concentration field and reflect all effects from local hydrogen stratification.

GASFLOW II includes models for plate and/or box recombination. A brief description of these models will be given and the results from validation calculations with these models will be presented. Table 1 gives an overview over the discussed experiments their key parameters, the data they provide and the 3D GASFLOW models used for their analysis.

Table 1: Recombiner Tests and Test Data analyzed with GASFLOW

Test			Facility	Test Vol. [m3]	Rooms	Walls	Sensors	GASFLOW 3D Model	simulated transient
Plate Reco		HDR E11.8.1	steel sphere	9.5	1	insulated steel	global: p, local: T, H2, H2O, Tplate, Tvessel	cartesian 15x, 15y, 15z	1h
Box Reco	Siemens	GX4	BMC[1]	209	5	concrete	global: p, local: T, H2, H2O, vel. In overflow openings	cylindrical 11 r,28 φ,18 z	20 h
		GX6							8 h
		GX7[2]							10 h
	NIS	MC3		625				cylindrical 11 r,12 φ,18 z	4h

BMC[1] = Battelle Model Containment

[2]GX7 was a dual concept test (recombination and combustion) with one recombiner box and 5 ignitors activated in different rooms at various times

Plate Recombiners

The model for catalytic foils (plate recombiners) in GASFLOW (fig. 1) considers structure surfaces with a special structure material index to recombine hydrogen and oxygen from the fluid node adjacent to such structure. It removes mass and energy of oxygen and hydrogen from the fluid node ($\Delta H2$, $\Delta O2$), adds their heat of recombination (242 kJ/mol) to the heat conduction node on the surface of the structure (qrec), and returns 1 mole of steam per removed 1.5 moles of hydrogen and oxygen with the steam energy of the foil surface temperature ($\Delta H2O$). If not enough oxygen is available, the oxygen concentration controls the reaction rate.

1D Heat conduction into the structure and radiative and convective cooling of the structure surface (qrad, qconv) determine the structure surface temperature. GASFLOW applies an orthogonal grid. A fluid node can be bounded in the limit by up to 6 different catalytically coated structure surfaces (figure 1 gives two surfaces as an example). The structure underneath the catalytic foil is considered as

composite material with thermal conductivities and heat capacities that can differ in each heat conduction node. One can define so called walls, where hydrogen recombination, 1D heat

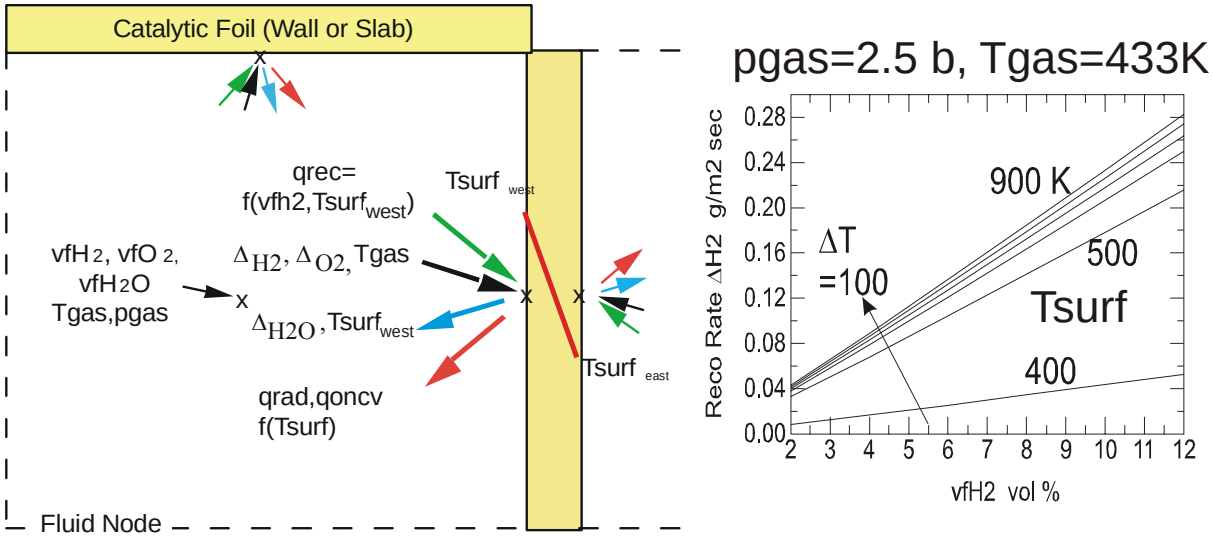

Figure 1: Catalytic foil model for hydrogen recombination in GASFLOW and applied correlation

conduction and heat exchange are simulated from both sides for a given number of heat conducting nodes in the wall. The walls are located on the boundaries of the computational mesh. They block the flow perpendicular to the mesh without taking away flow volume. The model also allows the definition of catalytically plated slabs. These are thicker structures, so called obstacles that take away flow volume from the 3D mesh. 1D heat conduction is simulated into these slabs which are generally quite thick. The heat flow into these structures is simulated in a 1D heat conduction mesh with a given number of mesh points and an inner boundary that is either adiabatic or kept at a given temperature. Modelling of 1D heat conduction into a multilayered material is a quite unique feature of GASFLOW which is not available in commercial CFD codes. The implemented algorithm identifies all recombining structure surfaces around a fluid node and recombines hydrogen proportional to the recombining surface areas that bound the fluid node.

The foil model has been developed for realistic containment geometries to treat catalytically coated structures that are represented in a coarse fluid mesh. The heat transfer is calculated with the Reynolds analogy between the momentum and thermal boundary layers from a logarithmic wall function applying a free slip flow boundary condition. Molecular and turbulent diffusion of hydrogen, oxygen and steam are simulated also in the coarse mesh. But the recombination rate on the catalytic foil is determined dependent on the hydrogen volume fraction (vfH2) and wall surface temperature (Tsurf) from experimental data because the mesh is generally too coarse near the wall. Figure 1 shows the applied correlation for the hydrogen recombination in HDR test E11.8.1 that was developed by Chakraborty [2]. The foil recombination is diffusion controlled and grows largely linear with the hydrogen concentration with only little dependence on the surface temperature in the temperature range of interest (Tsurf> 500K). Findings from foil tests in Jülich [3] suggest to neglect the temperature dependence of the recombination rate in such recombination processes because they are mostly diffusion controlled. In a simple geometry GASFLOW could directly simulate the hydrogen diffusion near such recombiner foils also in a first principle approach without experimental correlations. This would require a detailed wall treatment with full resolution of the boundary layer and a consistent description of momentum, heat and mass transfer to the catalytic foil with no slip conditions.

The radiative cooling of the hot foil surfaces is simulated with the radiation transport model from GASFLOW [4]. It calculates radiation transport through an absorbing emitting medium applying a P1 approximation for the direction dependent radiation intensity. The model calculates the radiation heat flux without view factors. It is applicable in arbitrary 3D geometries. But as is the case with neutron diffusion, which cannot be simulated in a vacuum, the model requires a certain radiation absorption in the gas. The model has been developed for an absorbing gas mixture with a sizeable steam content.

Test E11.8.1

The HDR test E11.8.1 with a catalytically plated foil was performed in an atmosphere with a high steam content. The spherical steel tank for the test had a volume of 9.5 m^3, was insulated on the outside and was initially filled with steam. A foil that was catalytically coated on both sides was eccentrically positioned in this tank. Air (8.5 Nm^3) from the top and then hydrogen (2.4 Nm^3) from the bottom were added to this steam atmosphere over 600 s and 400 s, respectively and the hydrogen and steam concentrations and the gas and foil temperature were measured for over an hour. The pressure increased from an initial 1.2 to 2.7 bar during the air and hydrogen injection and subsequently decayed from the reduction of the gas moles during the ongoing recombination (fig. 2).

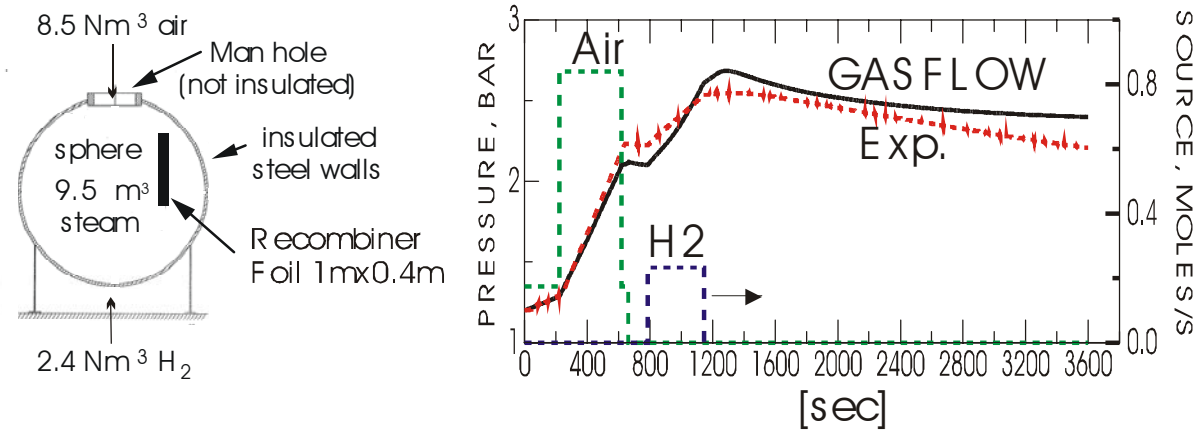

Figure 2: Catalytic foil HDR test E11.8. 1

GASFLOW simulated this experiment in a 3D Cartesian model for the tank with 15 nodes in the x-, y-, and z direction (3375 physical cells). The code predicts the measured gas pressure during the initial air and hydrogen injection into the steam atmosphere quite well. The steam volume fraction reduced from 100% to 60 % during the air-hydrogen injection. The gas mixture never became flammable.

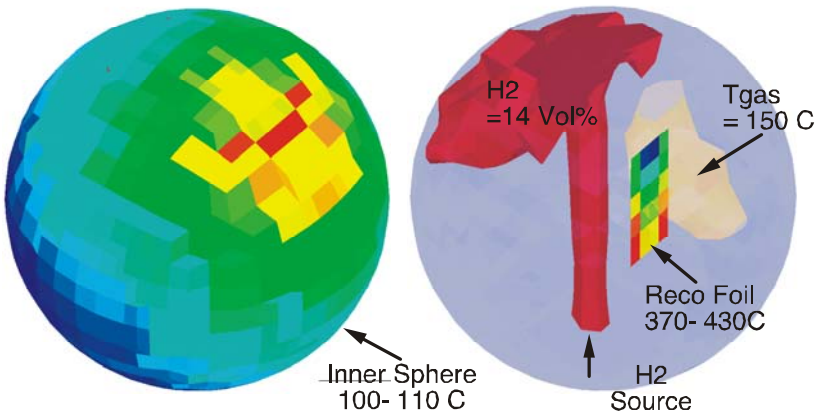

Figure 3: GASFLOW model for test E11.8.1 with snapshot at 1100 s

GASFLOW underestimates the pressure decay during the recombination. This is likely to come from the neglected heat loss through the manhole. We consid-

ered only the heat capacity of the steel tank with a thickness of 2 cm assuming an adiabatic outer boundary everywhere. Figure 3 shows the 3D-geometry model with the catalytic foil. Included is a snap shot with the calculated conditions at the end of the hydrogen injection at (1100s). Displayed are the calculated isosurfaces of the hydrogen cloud with 14 Vol%, the 150 C isosurface of the hot gas cloud around the catalytic foil and the temperature distribution on the foil surface.

Surface temperatures of the foil are indicated by the colored panels and vary from 370 to 430 C at this time. The foil is simulated as 24 wall panels that are catalytically active on both sides. 1D heat conduction is calculated through each panel using 20 heat conduction nodes. The thin plate (1 mm) with the high thermal conductivity of steel brings about identical temperatures on the front and back of each panel. Note that calculated foil temperatures are higher at the lower end and in the two outer columns of the panels which see higher hydrogen concentrations from both sides. The ongoing hydrogen injection forms a rising source jet that is deflected near the upper tank wall. Hydrogen rapidly mixes and diffuses into the containment atmosphere after the injection. The recombination reduces the hydrogen concentration near the catalytic foil. The jet deflection and the form of the gas temperature isosurface with 150 C indicate a downward circulation path on the right side of the foil that transports further hydrogen from the source jet to the foil while moving down some of the hot recombined steam. The tank temperature is indicated through the colored panels in the left of figure 3 and varies between 100 and 110 C. Radiative and convective heat transfer from the hot foil bring about higher tank temperatures above the foil and on the vessel side nearer to the foil with an asymmetric temperature distribution that is controlled by the simulated radiation transport.

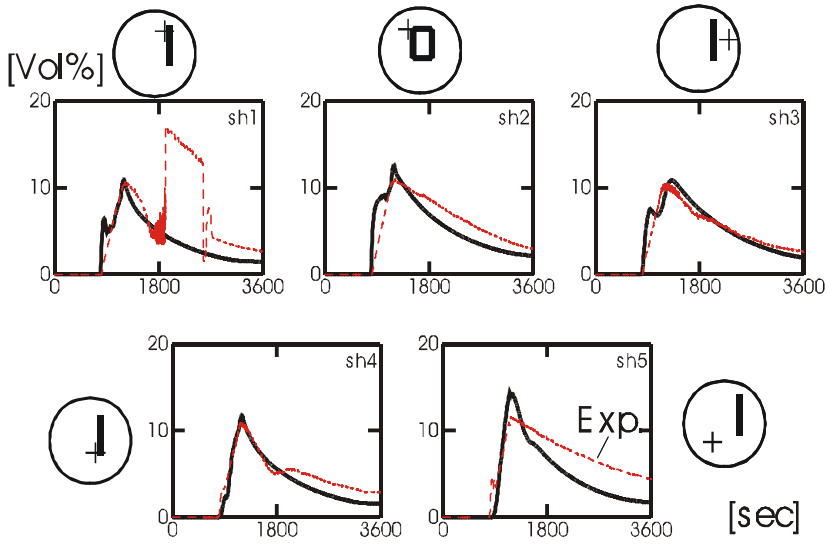

Figure 4: Hydrogen concentrations in test E11.8.1

The calculated and measured hydrogen volume fractions for test E11.8.1 are compared in figure 4 at the indicated sensor locations. The sensors sh1 and sh4 were located 10 cm away from the foil, the sensor sh5 on the other side near the axial midplane, 30 cm away. GASFLOW applied 10 cm fluid nodes adjacent to the foil surface. The calculated hydrogen concentration agrees quite well with the measured data, that peak around 12 Vol%. The good diffusion properties of hydrogen lead to a rapid atmospheric mixing in the calculation, which is also seen in the experimental data. An exception are the sensor data sh5 in the lower right that indicate a higher residual hydrogen concentration for the low location far away from the foil which is likely to come from hydrogen air sedimentation due to the steam condensation at the man hole. The measured surface temperatures on the recombiner foil peak at 600 C (fig. 5) The highest foil temperatures occur at the lower end of the foil (ft12). High surface temperatures are also measured at the upper end (ft8) where the increase occurs with some delay relative to the lower end. They can be explained with the calculated downward circulation from GASFLOW (fig. 3) and are in good agreement with the calculation. The two sensor data given for ft12 and ft8 refer to two symmetrically located thermocou-

ples.GASFLOW pictures the measured temperature peaks at the edges and near the axial midplane of the foil quite well with an emissivity value of 0.7 for the foil surface. Without radiative cooling the calculated foil surface temperatures would exceed 1000 C and be quite unrealistic. The calculated foil surface temperatures peak at similar values as the sensor data, but then all show a somewhat faster decay. GASFLOW simulated an ideally plane foil surface. The foil was actually coated by a fiber glass filter with an unknown surface and net porosity, which may allow for some trapping of the recombination energy and bring about some impedance to the radiation heat transfer. Radiative heat transfer is largely responsible for the calculated temperature increase on the tank surface (ft14) which is calculated to be only marginally above the sensor readings.

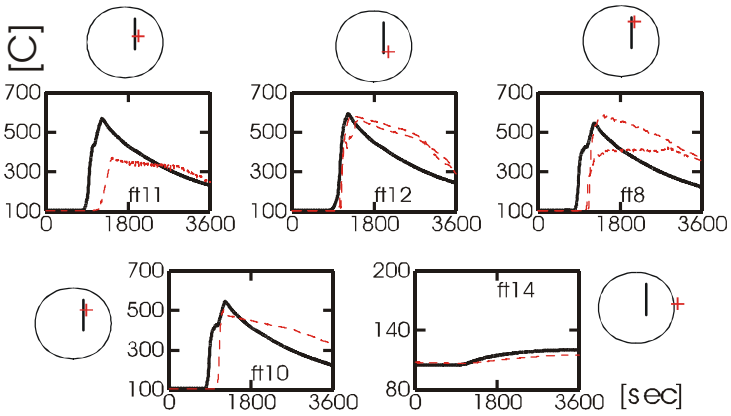

Figure 5: Surface temperatures of the recombiner foil in test E11.8.1

Further foil recombiner tests were planned within the Battelle Thincat program [5,6] to simulate the recombination on catalytically coated containment structures under realistic accident conditions. A full containment simulation with catalytic coating of insulation layers on primary pipings, pumps, steam generators and the pressurizer was performed with GASFLOW in preparation of these tests. Due to the large surface area of the catalytic foils more hydrogen could be removed than in a comparison case with recombiner boxes. But high structure surface temperatures with the potential for self ignition were predicted locally. They reduced strongly when the catalytic coating was applied on massive concrete or cooled steel structures instead of component insulations. A reduction of the hydrogen recombination was observed in containment regions with global downward convection. After cancellation of the Thincat program none of the questions raised from the scoping GASFLOW simulations with catalytic foils could be investigated further.

Box Recombiners

GASFLOW also models specific cells in the 3D mesh as recombiner cells. These cells are sepa-

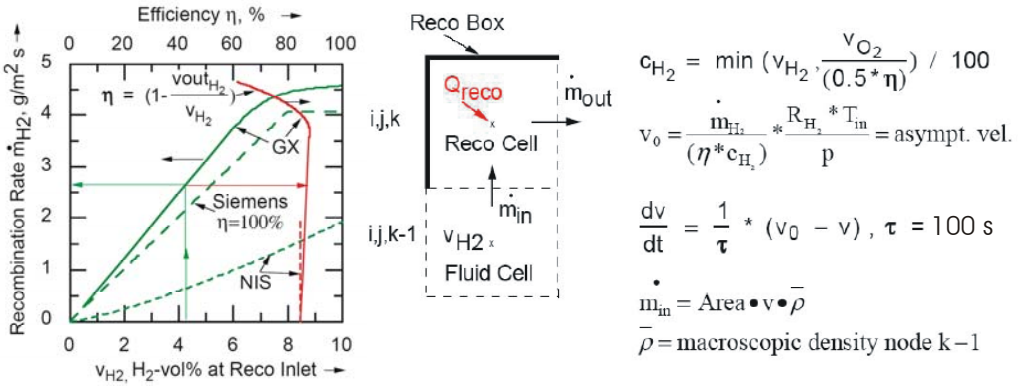

Figure 6: GASFLOW model for box recombiners (Siemens and NIS)

rated by walls from the adjacent fluid cells and have openings at the bottom for inflow and at the top or on the side for outflow (fig. 6). Measured performance data for boxes of the Siemens type containing arrays from catalytically coated plates and boxes of the NIS type containing a catalytic granulate have been implemented. They were derived under stationary conditions. Dependent on the local hydrogen concentration vH2 (with not enough oxygen also on the oxygen volume fraction vO2) below these cells gas is actively ventilated into these cells from below. The injection rate m_{in} is determined with a relaxation time constant τ from an asymptotic injection velocity v_0 that brings about the measured quasistationay recombination rate $m_{H2}$for the local hydrogen distribution at the entrance of the box. The constant R_{H2} is the gas constant of hydrogen, T_{in} and p are the pressure and the gas temperatures at the inlet of the box. The curves on the left of figure 6 show the measured performance data for a Siemens recombiner box from which the asymptotic injection velocity is determined. The solid green curve reflects the measured performance of the Siemens box recombiner FR90-150 that was tested in the Battelle GX experiments for near atmospheric conditions. The dashed green curve reflects the general performance for most Siemens recombiner boxes under operating conditions. It depends also on pressure. The hydrogen entering the box together with other gases is recombined according to a measured efficiency, the recombination energy Q_{reco} is added, gas cooling occurs inside the box on the walls with a specified heat capacity, and the hot gases m_{out} with steam and residual hydrogen are blown into the fluid mesh. The recombiner boxes are defined at appropriate locations in the 3D containment mesh and operate with local data from the 3D concentration field.

Experiments that tested the integral performance of both Siemens and NIS recombiner boxes under containment conditions in realistic accident scenarios with steam/hydrogen release have been performed in the Battelle model containment. (BMC). This model containment (fig. 7) is a cylindrical concrete building 9 m high and 11 m in diameter with a free gas volume of 625 m3. It has an outer zone with a dome and the annulus, and an inner zone with four annuli separated by concrete walls (so-called “banana rooms”) and one central compartment. Variable overflow openings allow the rooms to be combined into different chains of compartments.

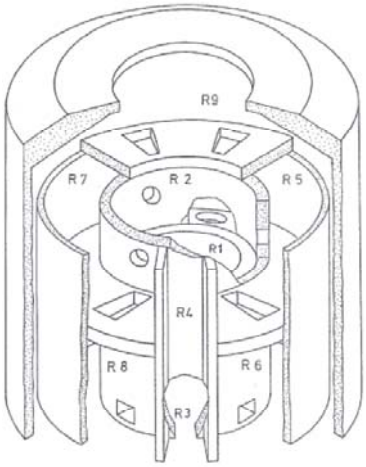

Figure 7: The Battelle Model Containment (BMC)

Test MC3

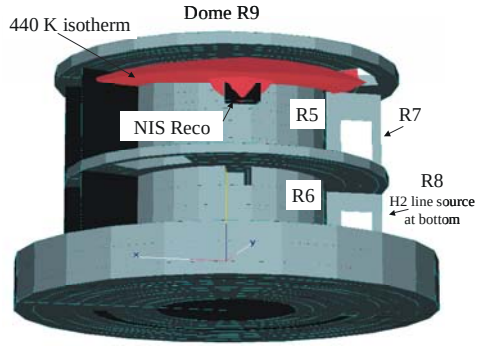

Figure 8: BMC test MC3 with NIS recombiner box and calculated exhaust plume at 10,000s

Test MC3 involved the entire Battelle containment. It tested the injection of hydrogen and the convection process in a steam/air atmosphere with hydrogen recombination through a full size NIS type granulate recombiner box [7]. The 3D snap shot in figure 8 shows the test configuration with the NIS recombiner box positioned near the ceiling on the inner wall of the bananaroom R5. The outer walls of the banana rooms have beeen intentionally left out in the figure also the outer containment walls and the top of the dome for display purposes. The GASFLOW analysis of test MC3 was performed in a 3D cylindrical model with 11 radial, 24 azimuthal and 18 axial meshes for the full facility. It

started without preconditioning using the measured initial steam concentration of 25 Vol% in the upper and 14vol% in the lower level and wall temperatures that are in thermal equilibrium with the gas temperature of the saturated steam/air mixture at 1 bar. A total of 3.5 kg of Hydrogen was then injected from a line source at the bottom of the banana room R8. It was released in two periods each of one hour with a one hour interval between the first and the second injection phase. The hydrogen distribution inside the containment was calculated. The unwrapped containment geometry in fig. 9 shows the pathes available for the hydrogen distribution in the multi room arrangement. The energy from the recombination at the NIS recombiner box became the dominant driving force for the atmospheric mixing and homogenization found in the containment during this experiment. The calculated hydrogen mass in the containment never exceeds 1 kg indicating that the recombiner is quite efficient in limiting the hydrogen concentration inside the containment. The high rate of recombination is also reflected by the hot plume above the recombiner box, that is displayed in fig. 8 as the 440 K isosurface. It imposes a significant thermal load on the ceiling. Most of the released hydrogen convects to the far end of the source room from where it is driven upward by buoyancy and drawn horizontally to the catalytic module in the adjacent banana room. The time evolution of the calculated hydrogen volume fractions at the recombiner inlet and exit are in good agreement with the measured data considering the large distance between the source and the recombiner through which the hydrogen has to convect. But the model lacks details in the startup phase (first 20 min) where it gives a somewhat too early start of the buoyancy pump from the exhaust gases. There is also a somewhat too slow reduction in the rate of hydrogen removal when the concentration reduces after the first pulse resulting in a lower hydrogen concentration at the beginning of the second pulse. Overall the analysis demonstrates well the ability to simulate hydrogen transport processes in large containment geometries in an integral approach that includes the pumping action and the species changes due to the recombiner box and that applies correlations for the recombiners that have been qualified with local test data. We have applied this box recombiner model in GASFLOW in the full containment analysis of a large break LOCA in Biblis A and demonstrated the strong mitigation effect of the positioning scheme with 42 NIS recombiners which the plant operator then installed in his facility [8].

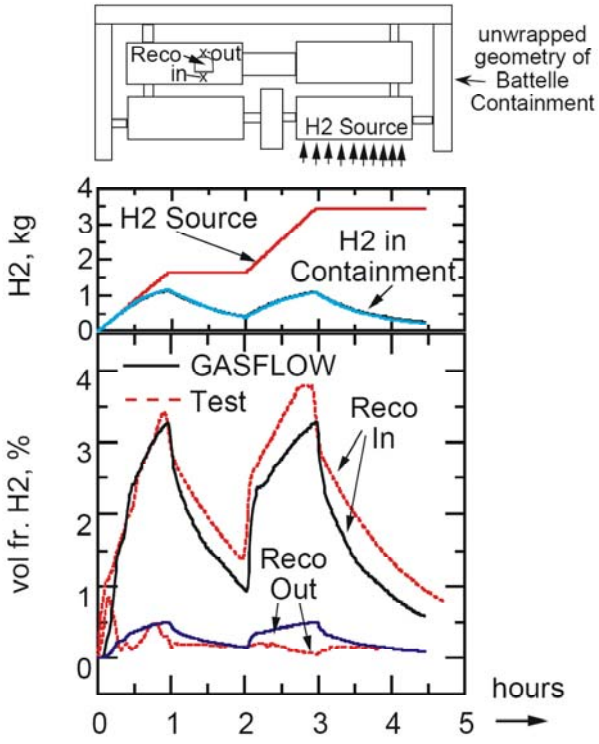

Figure 9: Hydrogen release and concentration at recombiner box in test MC3

Battelle GX tests

The GX series experiments that were also performed in the BMC tested one Siemens recombiner box under conditions of steam/hydrogen injection. They used a smaller recombiner box that was scaled from the large containment volume to the smaller test rooms of the BMC. They studied the influence of different release locations, different hydrogen release rates and different steam atmospheres.

So far the GX series are the only tests that also studied the combined mitigation effect of recombiners and igniters. Such combined mitigation measures of recombination and early ignition were discussed for some time as the so called "dual concept mitigation" when first designing for additional safety measures for severe beyond design accident scenarios . We have analyzed tests GX4, GX6 with the recombiner and test GX7 with the recombiner and the igniters using GASFLOW. Different from test MC3 where we started from measured initial conditions prior to the hydrogen injection, analysis of the GX tests started in an air filled containment from cold initial conditions and involved the full preconditioning of the containment atmosphere and concrete structures.

The GX tests were performed in the annular compartments R5 to R8 ("banana rooms") and the central cylindrical room R1/R3 of the BMC. A plug on top of the central room R1/R3 and closed openings on the outside of the banana rooms sealed off this inner containment from the annulus and the dome of the BMC. The total gas volume of the participating rooms was 209 m**3, each banana room R5 to R8 had a volume of 49 m**3. A radial cut and the azimuthally unwrapped banana rooms (fig. 10) show the arrangement of the test compartments. The recombiner box is positioned next to the inner wall of R5 not far from the overflow opening to R6 underneath. Steam is injected into R5, R6, and R8. Sump valves in each room are opened during certain phases of the test to limit the pressure increase and blowers in R5, R6, and R8 help to distribute the injected steam during the injection. Hydrogen can be injected from line sources at the bottom of R5 and R8. The blowers are shut off and the sump valves are generally kept closed during the hydrogen injection. Spark plug igniters are positioned in each compartment. They operate with a 7 s spark frequency, but are only selectively turned on during certain time intervals in the dual concept test GX7. Instrumentation of the GX tests was designed for lumped parameter simulations and only provided one data point for each room at the sensor locations indicated in figure 10.

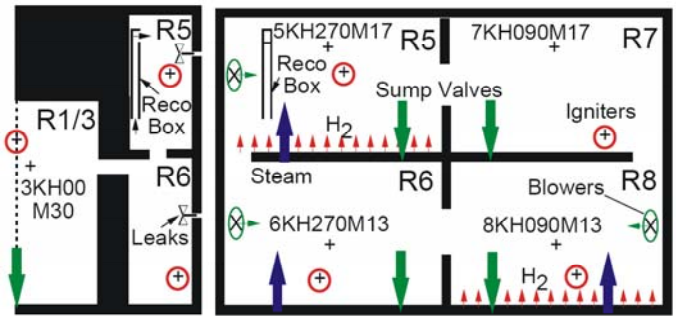

Figure 10: Arrangement of compartments and test setup in the Battelle model containment for the GX tests

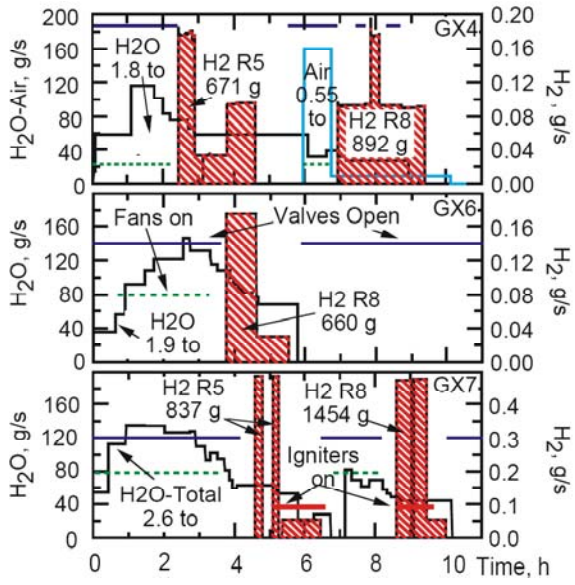

Figure 11: Steam/hydrogen sources blower times, and periods of igniter activation in the Battelle GX tests

Tests GX4 and GX6

The recombiner test GX4 involved two periods of hydrogen injection (fig. 11). The first one released 671 g hydrogen on the floor of room R5, the second 892 g into the bottom room R8. Test GX6 had only one injection period into R8 with 660 g of hydrogen. Initially we wanted to directly

simulate the recombination sequences during and right after each period of hydrogen injection starting with the measured gas temperatures and concentrations at the beginning of the different injection periods. Such a procedure would also have followed the grouping of the test data [9]. But the results were not satisfying because we could not specify the temperature profiles in the concrete structures consistently. This profile must reflect the thermal history of the pre-conditioning. We then started the calculation from cold isothermal conditions using the steam injections into the various compartments, the fan operation times and the opening periods of the sump valves as recorded in the experiments. In test GX4 ca. 50% of the steam were released in the upper room R5, while in test GX6 steam release was nearly evenly distributed between R5, R6, and R7. Both tests had a similar overall steam injection, but the earlier start of hydrogen injection initiated the recombination in GX4 around steam volume fractions of 27 % which were 10% lower than in test GX6.

We developed a cylindrical 3D GASFLOW model for the test geometry with 5852 computational cells with source reservoirs for steam and hydrogen in the floor of R5 and on the floor and in the inner wall of R8. Internal reservoirs with a constant pressure were also included to simulate the sump valves. These constant pressure reservoirs were disconnected by a zero velocity boundary during valve closure. We simulated the blowers using the option for a velocity boundary condition internally within the fluid mesh. All tests were performed with the same Siemens recombiner module. The geometry of the recombiner box (11.6 by 16 cm with a height of 1.6 m) was matched by adjusting the mesh. Seven axial meshes simulated a 1D axial flow inside the recombiner box . Comparison calculations demonstrated nearly the same results in a simulation with only one instead of 7 axial meshes for the recombiner box [10]. Walls with openings were defined that separate the recombiner box from the remaining fluid zones and heat exchange through the walls with the surrounding fluid cells was simulated. The buyoancy driven axial flow from the recombination was redirected into a radial flow at the exit of the box. The flow rate was determined from the hydrogen volume fraction below the recombiner inlet with the measured performance data of this box in fig. 8. We selected a small value of 100 s for the time constant τ that reflects the rather small thermal inertia of the Siemens recombiner plates relative to the NIS granulate recombiners for which we had applied a time constant of 1800 s. In agreement with the experimental data the flow through the recombiner box was initiated after the value of the hydrogen volume fraction at the recombiner inlet exceeded a value of 3%.

We compared the measured and the calculated hydrogen volume fractions from GASFLOW in each room at the indicated sensor locations in figure 12. The room is always indicated by the first digit in the sensor name.. The agreement is quite good. During the second injection period of GX4 with the hydrogen source in R8 GASFLOW somewhat overpredicts hydrogen concentrations in R5 and R7 and gives a somewhat lower concentration in the low source room R8. The concentrations in GX6 are right on the measured data. An exception is a small interval near 6 h between the end of the steam injection and the re-opening of the sump valves. A lot of air (57% of the initial mass) has been flushed out of

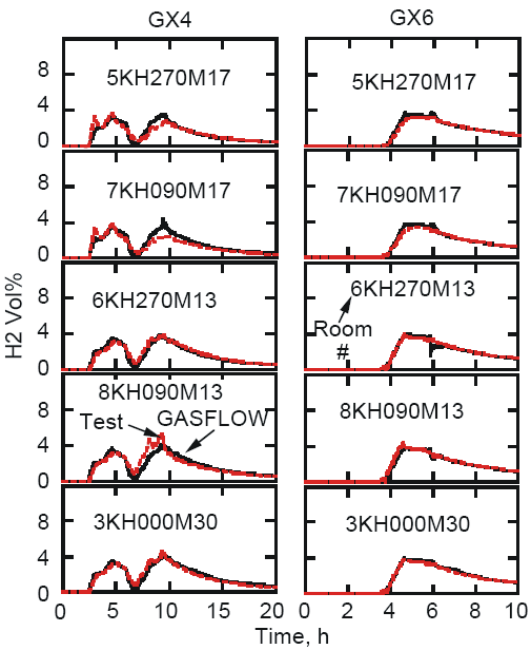

Figure 12: Measured and calculated hydrogen volume fractions in the GX4 and GX6 tests

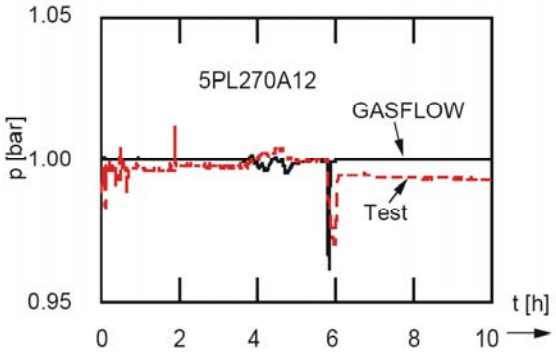

Figure 13: Measued and calculated pressure test GX6

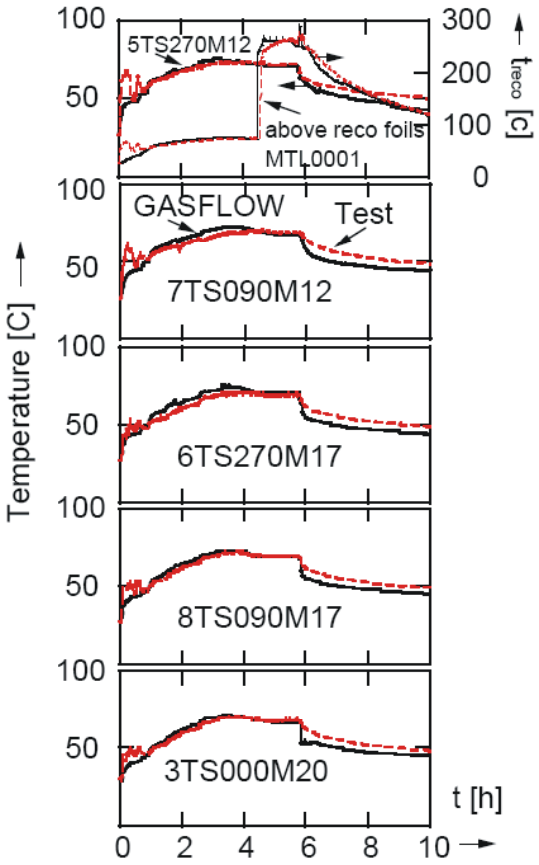

Figure 14: Measured and calculated temperatures test GX6

the containment through the open sump valves during the steam injection and recombination has further increased the steam volume fraction in the upper rooms by this time. GASFLOW simulates leak tight rooms during closure of the sump valves and consequently reduces the pressure from steam condensation after cutting off the steam source (see fig. 13). Condensation results in a temporary increase of the hydrogen volume fractions in R5 and R7 which have a higher steam content. This increase is also visible in the test data. When the sump valves open and the pressure returns to atmospheric conditions air is drawn through the valves in the floors which results in the temporary reduction of the hydrogen volume fraction visible from the results for R6. The volume fraction rises back to the measured values right after the pressure has returned to atmospheric conditions. The containment is not leak tight during valve closure. Therefore the measured pressure has a weaker reduction when the steam source is cut off prior to valve opening in GX6 near 6 h. But the calculated pressure reduction from the steam condensation in GASFLOW becomes also stronger because it starts from higher steam concentrations in the upper rooms where the calculated steam temperature is around 5 C higher than the test data. This explains also the stronger than measured temperature reduction which GASFLOW predicts during the pressure loss from steam condensation. Figure 14 compares the measured thermocouple data in each room. It also shows data from one sensor reading calculated inside the box at some distance above the recombiner plates. The earlier discussed slight over prediction of the hydrogen concentration in the upper rooms around the second injection period of GX4 is also tied to the reduction of the steam source. GASFLOW again predicts a too strong condensation effect then, that increases the hydrogen concentration locally and enhances the convection from the source room R8.

Test GX7

Test GX7 with recombiners and igniters involved higher steam and hydrogen releases than GX4 and GX6 (fig. 11). At some times even burnable mixtures occurred. Hydrogen again was injected in two periods, first from the top and then from the bottom. Spark igniters with a sparking time of 1 ms and frequency of 7s, which were installed in each compartment, were activated part of the time during hydrogen injection. Their activation times are indicated in figure 11. All analyzed GX tests proved the

existence of leakages. In test GX7 these leakages influenced the concentrations and pressure developments so much that leakages were simulated around the 14 instrumentation tubes penetrating the outer wall of the banana rooms as indicated in fig. 11. The leakage area taken into account in the analysis of GX7 totaled 43 cm2; the hydraulic diameter used was 1 mm.

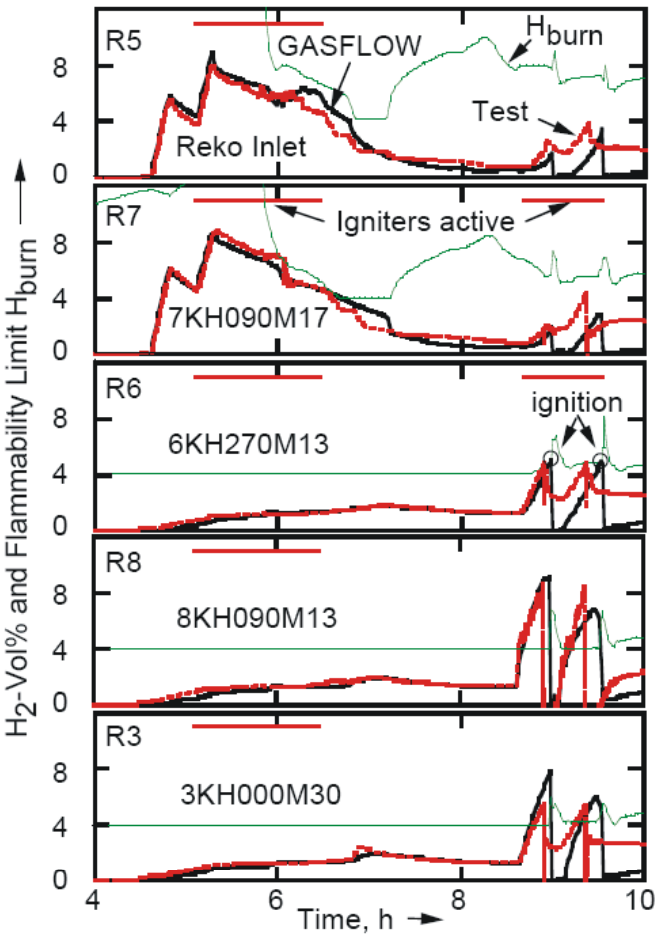

Figure 15: Measured and calculated hydrogen volume fractions, flammability limits, and ignition intervals in test GX7

The concentrations calculated for the different compartments of the GX7 experiment are shown in figure 15. The first hydrogen injection into the upper compartment, R5, causes pronounced stratification with maximum hydrogen concentrations of 8%. The high concentration spreads azimuthally also into the adjacent compartment R7, while concentrations in the lower compartments and in the central compartment increase very little.This stratification is rendered well by GASFLOW. The horizontal bars in figure 15 mark the activation periods of the igniters in various compartments. During the first hydrogen injection all igniters were activated. Despite the high hydrogen concentrations in the upper compartments, however, there was no ignition. The steam content was too high. The ignition limit of the hydrogen/steam/air mix, evaluated for the steam concentration in each room from the Shapiro diagram [11] (thin line in fig. 15), is above the hydrogen concentration throughout the first ignition phase. In the beginning the atmposphere is even completely inerted by steam (steam fraction > 65 Vol%). With decreasing steam injection, the steam fraction is reduced as a result of condensation; consequently the ignition limit in compartments R5 and R7 approaches the hydrogen concentration. The hydrogen concentration can even exceed the ignition limit briefly in compartment R7, but igniters are no longer active at this point in time. Also in the experiment there were no ignitions during the first hydrogen injection phase. All hydrogen associated with the first injection phase is reduced solely by the recombiner, which is active far below the ignition limit. Catalytic recombination causes the hydrogen content in the upper compartments to drop even below that in the lower compartments. Also in this late phase, the analysis reflects the experimental findings quite well.

The second injection of hydrogen occurs after 8.5 h down into compartment R8. Because of the low steam content in the lower compartments, the ignition limit is exceeded there very quickly. However, during the second hydrogen injection , no igniters were activated in the source compartment R8. During the second hydrogen injection, igniters were active only in the two adjacent compartments R6

and R7. As a consequence of the azimuthal hydrogen distribution, ignition conditions are established first in the horizontally adjacent compartment, R6. Ignition was very mild. In the simulation, flame propagation towards the source was initiated only by a considerable extension of the duration of the sparks because of the relatively coarse mesh grid for a combustion. The flame generated this way burns practically all of the hydrogen in the containment. In the experiment, only the source compartment, R8, burns out completely, while quenching goes on in all adjacent compartments so that a residual concentration of hydrogen is left. Hydrogen injection continues also after the first combustion. Again, the ignition limit is exceeded in compartment R6, and there is another ignition. Because of the absence of residual hydrogen, this occurs slightly later in the GASFLOW analyses than in the experiment. In GASFLOW, again all of the available hydrogen is burnt while residual concentrations in the adjacent compartments remain in the experiment. On the other hand, the code is able to describe the most important part of the combustion processes quite well, despite the lack of detailed models for the quenching process. The simulation of early ignition as a countermeasure preventing the buildup of mixes capable of detonation does not require excessive accuracy, e.g. with respect to the load potential. What is important is the local conservation of combustion enthalpy and its impact on convection in the containment. The analyses are sufficient in quality to meet these requirements.

Some analyses of the GX7 experiment reveal pronounced three-dimensional effects. This is indicated by the snapshots of two configurations in figure 16. The left side displays the status at the peak hydrogen concentration during the first hydrogen feed period. The status at the right is shown at the onset of the first ignition during the second hydrogen injection. Several results were superimposed in one diagram as different plumes. What is shown is the cylindrical model of the inner Battelle containment without the outer walls and the ceiling so as to provide a better view of the results. The hydrogen plume with concentrations above 9% is at the peak of the first hydrogen injection above the line source at the bottom of compartment R5. As a consequence of the continuous recombination effect, it is interrupted below the recombiner box. The hot offgases arising as a consequence of the recombina-

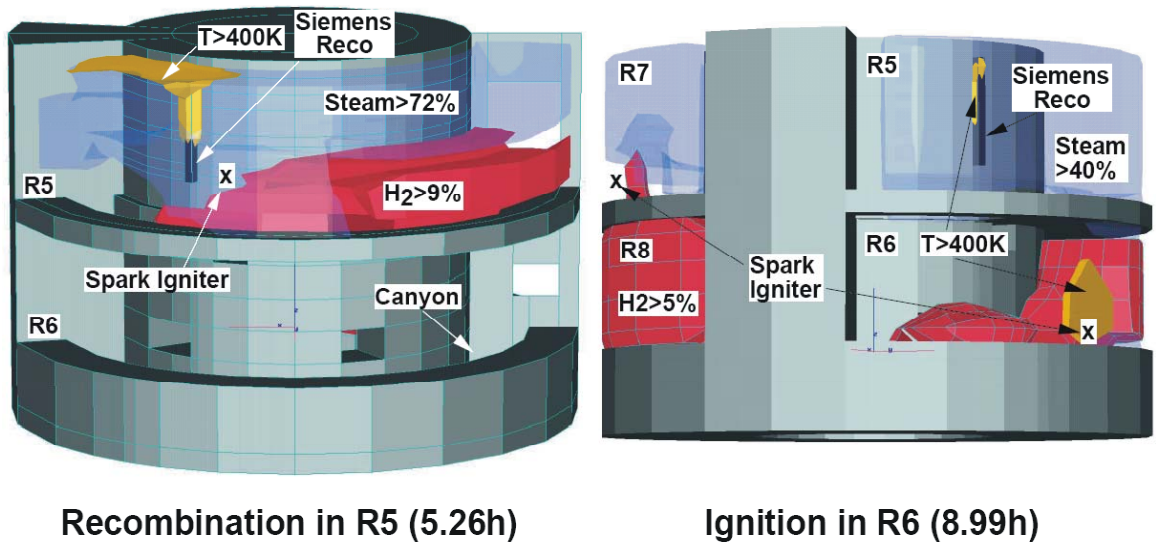

Figure 16: Snapshots at peak hydrogen concentration (left) and the onset of hydrogen ignition (right) in the GX7 test

tion energy are indicated by the isosurface above the recombiner, which encompasses the hot plume with gas temperatures above 400K. The blue transparent plume marks the region with steam volume percentages above 72%, indicating the steam inerted region in which no ignition is possible. This region extends throughout the upper regions of compartments R5 and R7, but not as far as the floor. The

igniter in R5 is situated fully in the region inerted with steam. If the igniter position in compartment R5 were different, for instance, a short distance above the floor, ignitions would have been possible even during the first injection phase. Local concentrations may vary greatly even in this small compartment.

The first ignition after nine hours produces a completely different picture. The geometry model was turned slightly counter clockwise to allow the onset of ignition to be indicated and to clear the view of the R8 source compartment and the R6 ignition compartment. A hydrogen plume with hydrogen concentrations above 5% extends into the entire source compartment R7, R8, and in an azimuthal direction also into the R6 compartment. A finger of the plume in compartment R7 indicates that hydrogen was able to penetrate locally also into the upper compartment. Another plume is generated at the lower connection between R6 and and the central compartment, R3. It is produced as a result of dispersion via the central compartment. The transparent blue plume now marks the region with steam volume fractions above 40%. The steam volume fraction in the upper compartments is higher; at the overflow opening from R8 to R7 the propagating hydrogen plume has displaced the steam locally. At the onset of ignition, the steam fraction is below the inerting limit of 65% throughout. The crosses in compartments R7 and R6 indicate the positions of the two igniters active in the second hydrogen injection phase. Ignitable mixtures are produced at first at the igniter in R6. The plume above the igniter marks the hot gas region at T>400K established locally after the first ignition. The recombiner continues to operate also in this phase. Because of the much lower hydrogen concentration in the R5 compartment, its offgas plume is only weak. After the ignition the flame propagates along the gradient of rising hydrogen concentrations. This process involves branching into an azimuthal propagation towards the source and into a flame front moving through the central compartment towards the source compartment. When the two flame fronts meet in the source compartment there is a brief pressure peak which, compared to the measured data is overestimated in the GASFLOW analysis (narrow pressure peak of 1.9 bar as against a measured broader peak of 1.3 bar. The calculated transient flame propagation after ignition was visualized as a film.

Conclusions

The 3D field code GASFLOW can give reliable predictions of steam/hydrogen distributions with mitigation by catalytic hydrogen recombiners also in complex containment geometries. This was also shown with the successful interpretation of various other thermal hydraulic tests on different scales [12] which validated our code and gave confidence to our 3D full containment applications with mitigation by NIS and Siemens recombiner boxes. The discussed analyses demonstrate the flexibility of the box model to cope with modifications of the recombiner designs. Most of the analysed recombiner experiments were performed 10-15 years ago and the results were known, thus none of these calculations was made blindly. Instrumentation of most tests was developed for analysis with coupled volume models rather than for CFD codes. But the available data are of a high quality also for the analysis with CFD codes although their quantity is limited compared to the instrumentation installed in new modern test facilities. Velocity data on steam hydrogen distribution with mitigation that could be compared with CFD results are not available. Most recorded and compared data are temperatures and volume fractions of steam and hydrogen. All except one of the analysed tests were performed at near atmospheric pressures. The prediction of small pressure variations during the tests was difficult and overshadowed by the leakage of the concrete containment. Three dimensional CFD calculations were not really necessary for the analysis of tests MC3, GX4, and GX6 with good atmospheric mixing. But the demonstration how this mixing was achieved in a 3D CFD analysis also gave confidence to the predictions. Test GX7 was probably the most challenging test. It showed up a real 3D behaviour, which could never be captured in a coupled volume approach. Its successful interpretation with

GASFLOW provided a deeper understanding of the test data and controlling phenomena think alone of the sensitive local interplay between steam and hydrogen concentration with recombination and ignition found during the different hydrogen injection phases of this test. This could only be shown up by the CFD simulation because not sufficient sensor data were available to gain such deeper understanding. Test E11.8.1 with catalytic foils was better instrumented and did not have any of the leakage problems of the Battelle containment. But in this test an insufficient insulation of the test vessel at the man hole was difficult to model which disturbed the steam condensation somewhat. The satisfactory prediction of the foil surface temperatures in this test also validated the radiation model implemented in the code.

References

[1] J. R. Travis, J. W. Spore, P. Royl et al.:"GASFLOW a computational fluid dynamics code for gases aerosols and combustion, FZKA-5994 Vol I-III, October 1998

[2] S. G. Markandeya, A. K. Chakraborty:"Modelling of Catalytic Recombiners for Removal of Hydrogen during Severe Accidents:, Procs 12th SMiRT Conference Paper U04/3 Stuttgart 1993

[3] P. Bröckerhoff, E.-A. Reinecke:"Untersuchungen zur Auslegung Katalytischer Rekombinatoren:, Procs. Jahrestagung Kerntechnik, Bonn 2000

[4] J. R. Travis:"A Computationally Efficient Thermal Radiation Transport model for the GASFLOW Code", Procs 15th SMiRT Post Conference Seminar on Containment of Nuclear Reactors, Seoul, Korea, August 23-24 1999

[5] K. Fischer, P. Bröckerhoff, G. Ahlers, V. Gustavsson, L. Herranz, J. Polo, T. Dominguez, P. Royl: „Hydrogen removal from LWR containments by catalytic-coated thermal insulation elements (THINCAT)", Nuclear Engineering and Design 221 (2003) 137-149

[6] P. Royl, J. R. Travis, W. Breitung : "Modeling of catalytic foils and application in 3D containment analysis", Procs. IAEA Technical Committee Meeting, Cologne, 18-22 June 2001, Report IAEA-J4-TC-1181

[7] M. Eigenbauer, M. Seidler:"Entwicklung eines Systems zum katalytischen H2-Abbau nach auslegungsüberschreitenden Störfällen in Kernkraftwerken", NIS Ingenieurgesellschaft Hanau, Technischer Bericht Nr. 1141/1866/0 (1991)

[8] P. Royl, H. Rochholz, W. Breitung, J. R. Travis, G. Necker:"Analysis of steam and hydrogen distributions with PAR mitigation in NPP containments", Nuclear Engineering and Design 202 (2000) , 231-248

[9] T. Kanzleiter: "Versuche zur Wirksamkeit von Wasserstoff-Gegenmaßnahmen in einer Mehrraum-Containment-Geometrie", Battelle Insitut e.V., Frankfurt/M, März 1991

[10] Royl, P., Necker, G., Spore, J. W., Travis, J. R.:"Validation of Coarse Catalytic Recombiner Models in the 3D Field Code GASFLOW with Battelle GX Tests for the Analysis of Large Containments", Procs. Jahrestagung Kerntechnik, München, 1998

[11] Z. M. Shapiro, T. R. Moffette:"Hydrogen Flammability Data and Application to PWR Loss-of-Coolant Accident", WAPD-SC-545, Bettis Plant, 1957

[12] Royl, P., Travis, J. R., Breitung, W. :"Benchmarking of the 3D CFD Code GASFLOW II with containment thermal hydraulic tests from HDR and ThAI", these Proceedings